

1

Introduction to Nuclear Magnetic Resonance

Two groups lead, respectively, by Bloch and Purcell discovered almost simultaneously the phenomenon of nuclear magnetic resonance (NMR). Bloch and Purcell shared the Nobel Prize for physics in 1952.

NMR is the most powerful method for the identification of organic compounds, and is widely applied in many fields.

In this chapter, the basic principles and concepts of NMR spectroscopy are described. Discussions on ^1H spectra, ^{13}C spectra and 2D NMR spectroscopy will be given in Chapters 2, 3 and 4, respectively.

References 1, 2 are provided for the reader who would like to have a further understanding of the basic concepts of NMR spectroscopy.

1.1

Basic Principle of NMR

1.1.1

Nuclear Magnetic Momentum

Magnetic nuclei are the objects studied by NMR. The atomic nucleus consists of neutrons and positively charged protons so that a nucleus can possess magnetic momentum when it “spins” about the nuclear axis. The spinning motion of a nucleus is determined by spin quantum number I . There are three different cases:

1. A nucleus with an even number of neutrons and an even number of protons has a zero spin quantum number, for example, ^{12}C , ^{16}O , ^{32}S and so forth.
2. A nucleus with an odd number of neutrons and an even number of protons, or with an even number of neutrons and an odd number of protons, has a half-integral spin quantum number, for example:
 $I = 1/2$, such as ^1H , ^{13}C , ^{15}N , ^{19}F , ^{31}P , ^{77}Se , ^{113}Cd , ^{119}Sn , ^{195}Pt , ^{199}Hg , and so forth.
 $I = 3/2$, such as ^7Li , ^9Be , ^{11}B , ^{23}Na , ^{33}S , ^{35}Cl , ^{37}Cl , ^{39}K , ^{63}Cu , ^{65}Cu , ^{79}Br , ^{81}Br and so forth.
 $I = 5/2$, such as ^{17}O , ^{25}Mg , ^{27}Al , ^{55}Mn , ^{67}Zn and so forth.
 $I = 7/2$, $9/2$ and so forth.

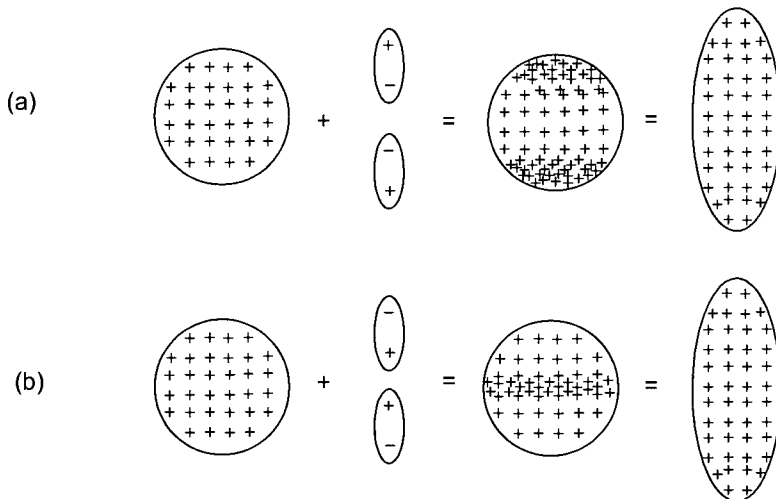


Fig. 1.1 Non-uniform distributions of nuclear charges and electric quadrupole moments.

3. A nucleus with an odd number of neutrons and an odd number of protons has an integral spin quantum number, for example: $I=1$ for ${}^2\text{H}$, ${}^6\text{Li}$, ${}^{14}\text{N}$; $I=2$ for ${}^{58}\text{Co}$; $I=3$ for ${}^{10}\text{B}$.

From the above, it follows that only nuclei belonging to cases 2 and 3 are the objects that can be studied by NMR. Those nuclei which have a non-zero spin quantum number are called magnetic nuclei. Furthermore, only the nuclei with $I=1/2$ are suitable for NMR measurement because they have a uniform charge distribution over the nuclear surface. As a result, they have no electric quadrupole moment (see below) so they can be recorded as narrow peaks in their NMR spectra. On the other hand, all other magnetic nuclei (with $I>1/2$) have a non-uniform charge distribution over the nuclear surface, as shown in Fig. 1.1, which leads to broadened peaks in their NMR spectra.

The distribution shown in Fig. 1.1a can be considered as the addition of a uniform charge distribution and a pair of electric dipoles, whose negative “poles” are towards the nuclear “equator”, which leads to the concentrated positive charge distribution at two nuclear “poles.” If the nucleus extends longitudinally to give a uniform charge distribution, it has a positive electric quadrupole moment according to the following equation:

$$Q = (2/5)Z(b^2 - a^2) \quad (1-1)$$

where Q is the electric quadrupole moment of the spheroid; b and a are the half longitudinal axis and the half transverse axis, respectively; Z is the charge carried by the spheroid.

Similarly, the distribution shown in Fig. 1.1b possesses a negative electric quadrupole moment.

All nuclei with an electric quadrupole moment (positive or negative) have a specific relaxation mechanism, which leads to a rapid relaxation so as to broaden their peaks. This is why only the nuclei with $I=1/2$ are suitable for NMR measurement.

The nucleus with a non-zero spin quantum number has an angular momentum, P , the magnitude of which is given by Eq. (1-2):

$$P = \sqrt{I(I+1)} \frac{h}{2\pi} = \sqrt{I(I+1)} \hbar \quad (1-2)$$

where h is Planck's constant:

$$\hbar = \frac{h}{2\pi}$$

The nucleus with an angular momentum has a magnetic moment, given by Eq. (1-3):

$$\mu = \gamma P \quad (1-3)$$

where γ is the constant of proportionality relating μ and P , known as the magnetogyric ratio, which is an important property of the nucleus.

1.1.2

Quantization of Angular Momentum and Magnetic Moment

According to quantum mechanics, when a magnetic nucleus is placed in a static magnetic field B_0 , which is along the z direction, the angular momentum of the nucleus is quantized and it will adopt one of $(2I+1)$ orientations with respect to the external magnetic field. The allowed projections of the angular momentum on the z axis, P_z , are confined to several discrete values, which are given by Eq. (1-4):

$$P_z = m\hbar P_z = m\hbar \quad (1-4)$$

where m is the magnetic quantum number of the nucleus. It has $2I+1$ values, $m=I, I-1, I-2, \dots, I$.

The quantization of angular momenta in a static magnetic field is shown in Fig. 1.2.

The projections of magnetic moments of the nucleus on the z axis, μ_z , are given by Eq. (1-5):

$$\mu_z = \gamma P_z = \gamma m\hbar \quad (1-5)$$

When a nucleus is placed in a magnetic field B_0 , which is along the z axis, the energy of the nucleus is given by

$$E = -\mu \cdot B_0 = -\mu_z B_0 \quad (1-6)$$

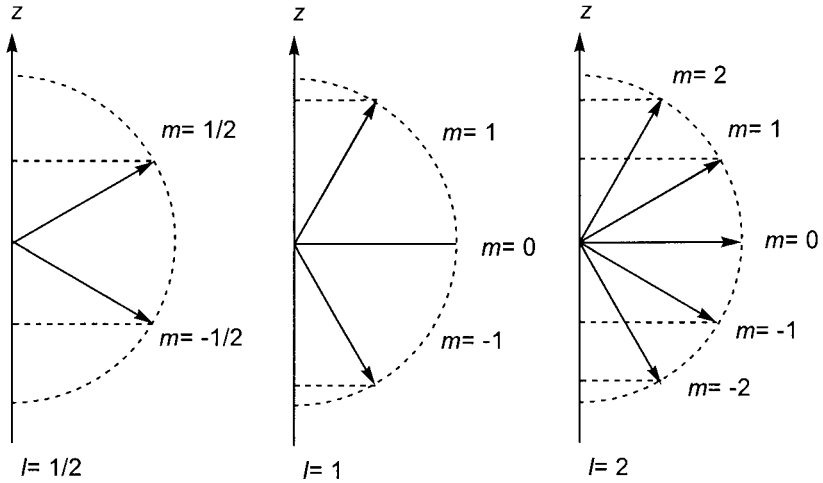


Fig. 1.2 The possible orientations for angular momenta.

Substituting Eq. (1-5) into (1-6) leads to

$$E = -\gamma m \hbar B_0 \quad (1-7)$$

Thus, the energy differences between various energy levels are

$$\Delta E = -\gamma \Delta m \hbar B_0 \quad (1-8)$$

According to the selection rule of quantum mechanics, only transitions with $\Delta m = \pm 1$ are allowable, so that the energy difference for allowed transitions is

$$\Delta E = \gamma \hbar B_0 \quad (1-9)$$

On the other hand, $m = I, I-1, \dots, -I$, that is, the magnetic moment has $2I+1$ orientations. Using Eq. (1-6), we obtain the energy difference for allowed transitions:

$$\Delta E = \frac{2\mu_z B_0}{2I} = \frac{\mu_z B_0}{I} \quad (1-10)$$

where μ_z is the maximum projection of μ on the z axis.

1.1.3

Nuclear Magnetic Resonance

There are various energy levels for the nucleus with a magnetic moment in a static magnetic field. The nucleus will undergo a transition if an electromagnetic wave with a frequency given by Eq. (1-9) is used. This transition is nuclear magnetic resonance (NMR). Thus the fundamental equation can be derived as follows:

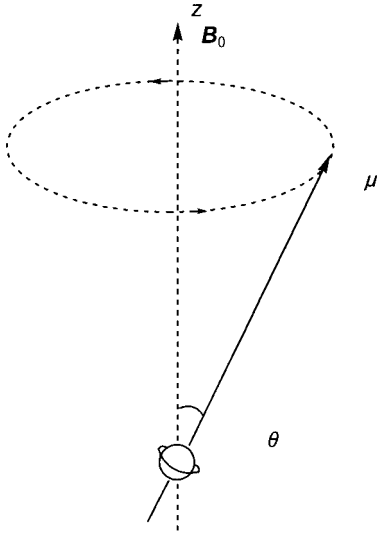


Fig. 1.3 A magnetic nucleus precesses in a static magnetic field.

$$h\nu = \gamma\hbar B_0$$

$$\nu = \frac{\gamma B_0}{2\pi} \quad (1-11)$$

where ν is the frequency of the electromagnetic wave. Its relevant circular frequency ω is

$$\omega = 2\pi\nu = \gamma B_0 \quad (1-12)$$

NMR can be discussed from another point of view. In a static magnetic field B_0 (along the z axis), a precession motion (also known as the Larmor precession) of a magnetic nucleus takes place because the nuclear spinning axis makes an angle θ with respect to the z axis, which is shown in Fig. 1.3. This situation is similar to that where a spinning gyroscopic top precesses when it is tilted with respect to the gravitational field.

The Larmor precession frequency ω_L is given by Eq. (1-13):

$$\omega_L = \gamma B_0 \quad (1-13)$$

Precession directions are determined by the sign of the γ .

Suppose that a linear polarized oscillating magnetic field, that is, an electromagnetic radiation, with the Larmor angular frequency ω_L is applied to the plane perpendicular to the static magnetic field B_0 . This magnetic field can be split into two components rotating in opposite directions. One of these components

Tab. 1.1 NMR properties of some magnetic isotopes

<i>Isotope</i>	<i>Resonance frequency*</i> (MHz)	<i>Natural abundance</i> (%)	<i>Relative sensitivity</i> (with respect to the proton at a fixed B_0)	<i>Magnetic moment μ</i> (multiply by $eh/4\pi mC$)	<i>Spin quantum number l</i>	<i>Electric quadrupole moment</i> ($e \times 10^{-24}$ cm)
^1H	42.577	99.9844	1.000	2.79270	1/2	–
^2H	6.536	1.56×10^{-2}	9.64×10^{-3}	0.85738	1	2.77×10^{-3}
^{13}C	10.705	1.108	1.59×10^{-2}	0.70216	1/2	–
^{14}N	3.076	99.635	1.01×10^{-3}	0.40357	1	2×10^{-2}
^{15}N	4.315	0.365	1.04×10^{-3}	–0.28304	1/2	–
^{17}O	5.722	3.7×10^{-2}	2.91×10^{-2}	1.8930	5/2	-4×10^{-3}
^{19}F	40.055	100	0.834	2.6273	1/2	–
^{31}P	17.235	100	6.64×10^{-2}	1.1305	1/2	–
^{33}S	3.266	0.74	2.26×10^{-3}	0.64274	3/2	-6.4×10^{-2}
^{35}Cl	4.172	75.4	4.71×10^{-3}	0.82089	3/2	-7.97×10^{-2}
^{37}Cl	3.472	24.6	2.72×10^{-3}	0.68329	3/2	-6.21×10^{-2}
^{79}Br	10.667	50.57	7.86×10^{-2}	2.0990	3/2	0.33
^{81}Br	11.498	49.43	9.84×10^{-2}	2.2626	3/2	0.28
^{127}I	8.519	100	9.35×10^{-2}	2.7939	5/2	–0.75

* Resonance frequency at 1 Tesla.

rotating in the opposite direction to that of nuclear precession is ineffective. The other component excites the nuclear precession because of the same direction of rotation and the same frequency. Some energy is transferred from the electromagnetic wave to the magnetic nuclei, which is NMR.

The NMR properties of some magnetic isotopes, which exist in organic compounds, are given in Tab. 1.1.

1.2 Chemical Shift

In 1950 Proctor and Yu found two NMR signals for a solution of ammonium nitrate. Clearly these two signals belong to ammonium ions and nitrate ions, respectively, that is, NMR signals can distinguish nuclei in different chemical surroundings for a given isotope.

1.2.1 Shielding Constant

The above-mentioned phenomenon can be explained by the shielding effect of the electrons surrounding the nuclei. The magnitude of the magnetic field actually experienced by the nuclei is slightly less than that of the applied field. Therefore, Eq. (1-11) should be modified as

$$\nu = \frac{\gamma}{2\pi} B_0(1 - \sigma) \quad (1-14)$$

where σ is known as the shielding constant or the screening constant. It is a field-independent factor and is related to the chemical surroundings of the nuclei. Different isotopes possess various σ values covering maybe several orders of magnitude, but σ values of all isotopes are much less than 1.

σ can be shown to be

$$\sigma = \sigma_d + \sigma_p + \sigma_a + \sigma_s \quad (1-15)$$

σ_d is the diamagnetic term, which is contributed by s electrons. The induced electron circulation produces a diamagnetic field. The term “diamagnetic shielding” arises from the fact that the induced field is opposed to the applied field. The greater the density of s electrons around the nucleus, the less field strength the nucleus experiences. Acted on by the shielding effect, the resonance peak of the nucleus will shift towards the right.

σ_p is the paramagnetic term, which is contributed by p and d electrons that are distributed unsymmetrically about the nucleus. Because of the hindrance by other chemical bonds, the direction of the induced field coincides with that of the applied field, hence the term “paramagnetic shielding.” σ_a indicates the anisotropic influences from neighboring groups and σ_s shows the solvent (or medium) effects.

The effects from σ_d and σ_p are much greater than those from σ_a and σ_s . σ_p is much more important than σ_d for all isotopes except ^1H .

1.2.2

Chemical Shift δ

For a given isotope, nuclei in various functional groups will show their NMR signals with different abscissas because of their different σ values. A specific substance is selected as an internal standard, the peak for which is set as the origin of an NMR spectral abscissa. All peak positions of functional groups of a compound are defined as

$$\delta = \frac{\nu_{\text{sample}} - \nu_{\text{standard}}}{\nu_{\text{standard}}} \times 10^6 \quad (1-16)$$

where ν_{sample} and ν_{standard} are the resonant frequencies of the functional group and the standard, respectively.

δ , known as the chemical shift, shows the peak position for a particular functional group and is in ppm (parts per million), which is dimensionless. Its sign is negative when a signal is positioned on the right side of the standard and positive when on the left side.

Since the numerator of Eq. (1-16) is far less than the denominator by several orders of magnitude, and ν_{standard} is very close to the nominal frequency of the NMR spectrometer, ν_0 , ν_{standard} is replaced by ν_0 .

Tetramethylsilane is usually applied as the standard because it has only a single peak and it can be easily removed from the sample (bp=27°C). An additional advantage is that common functional groups have positive δ values.

1.3 Spin-spin Coupling

In 1952, Gutowsky et al. reported that two ^{19}F peaks existed for a POCl_2F solution, which led to the discovery of spin-spin couplings.

1.3.1 Spin-spin Coupling Produces NMR Signal Splitting

The splitting of the ^{19}F signal is produced by ^{31}P being connected to ^{19}F . Because ^{31}P possesses a spin quantum number of $1/2$, it has two orientations with almost equal probabilities: either approximately parallel or anti-parallel to the applied magnetic field, which leads either to an increase or to a decrease in the magnetic field experienced by the ^{19}F . Consequently, the singlet corresponding to Eq. (1-14) is replaced by a doublet with a roughly identical intensity. This effect of producing the spin-spin splitting is known as spin-spin coupling, the magnitude of which, known as the coupling constant J and measured in Hertz, is measured by the space between adjacent split peaks in a multiplet. If more than one magnetic nucleus (with a spin quantum number of $1/2$) couples with another magnetic nucleus, the NMR signals of the nucleus to be coupled will show further splitting. The splitting pattern can be described by Pascal's triangle (Tab. 1.2), where n is the number of nuclei that participate in coupling. Multiplicity indicates the split signal of the nuclei to be coupled. The relative peak intensities of a multiplet are shown by the developed binomial coefficients in Pascal's triangle, from which the $n+1$ rule can be understood: $n+1$ peaks will be produced by the coupling of n nuclei.

Tab. 1.2 Pascal's triangle

n	Relative peak intensities Developed binomial coefficients	Multiplicity
0	1	singlet
1	1 1	doublet
2	1 2 1	triplet
3	1 3 3 1	quartet

1.3.2

Energy Level Diagram

The energy level diagram is very useful for theoretical discussions on NMR. An AX system, which consists of two coupled magnetic nuclei, will be used as an example. The details of spin systems will be described in Section 2.3.

Consider that both of the two nuclei have a spin quantum number of $1/2$, so each has two orientations with respect to the applied magnetic field. We use a to denote the orientation corresponding to the magnetic quantum number m of $1/2$ and β to that of $-1/2$. Consequently, four energy levels exist, which are $A(a) X(a)$, $A(\beta) X(a)$, $A(a) X(\beta)$ and $A(\beta) X(\beta)$, simplified as aa , βa , $a\beta$ and $\beta\beta$, respectively.

1. The energy level diagram without coupling between A and X.

The energy level diagram, which contains four energy levels, 1, 2, 3 and 4, according to the order of increasing energy, is shown in Fig. 1.4.

The transition from level 1 to level 2 changes the a state of the A nucleus to the β state without changing the X spin state, so the signal belongs to A. The same is true of the transition from level 3 to level 4. On the other hand, both the transition from level 1 to level 3 and that from level 2 to level 4 produce the X signal.

Because of the equal energy differences, there is only a peak for A and a peak for X.

Fig. 1.4b is usually used to give a clear demonstration.

2. The energy level diagram with coupling between A and X.

Because of the mutual actions between magnetic nuclei, the energy levels of the AX system will be changed when a coupling between A and X exists. Suppose that levels 1 and 4 are raised by a magnitude of $J/4$, and correspondingly, levels 2 and 3 will be decreased by the same magnitude. Consequently, on the basis of Fig. 1.4, a new energy level diagram, Fig. 1.5, is drawn, in which levels 1', 2', 3' and 4' are transferred from levels 1, 2, 3 and 4 of Fig. 1.4, respectively.

Related calculations lead to Fig. 1.6.

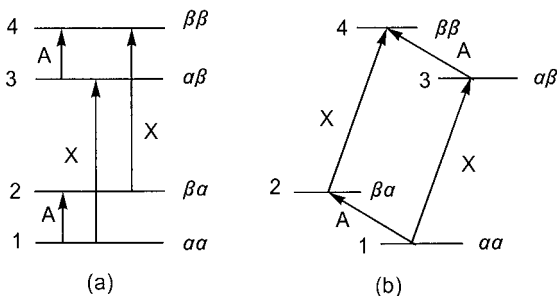


Fig. 1.4 The energy level diagram of an AX system without the coupling between A and X.

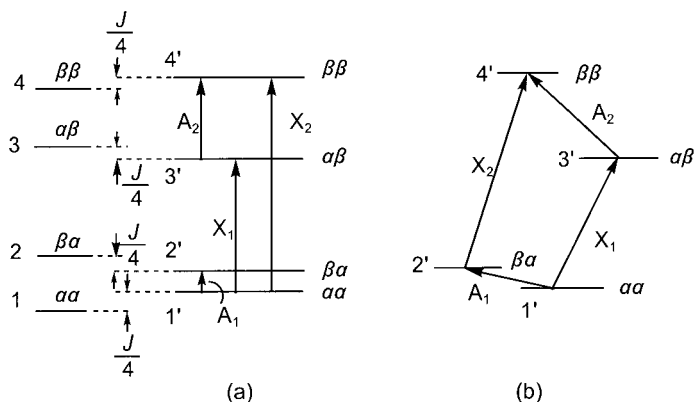


Fig. 1.5 The energy level diagram of an AX system with the coupling between A and X.

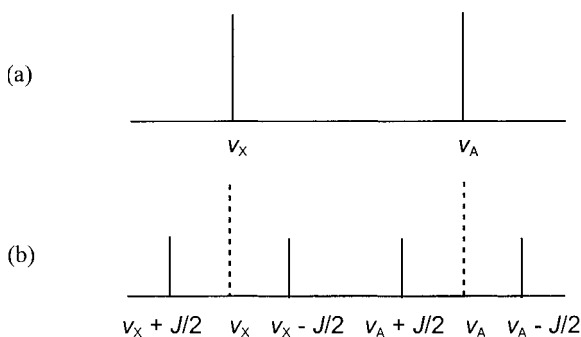


Fig. 1.6 The NMR spectrum of an AX system (a) without coupling between A and X (b) with coupling between A and X.

When a coupling between A and X exists, there are two sets of split peaks for A and X, respectively. Each set of peaks keeps the same δ value (measured at the middle point between the two peaks) because the coupling does not affect the chemical shift. Two peaks, which belong to one nucleus, are separated by a spacing, J . The two peaks have the same intensity. The coupling constant J , measured in Hertz, is independent of the applied magnetic field or the spectrometer frequency.

1.3.3

Coupling Constant J

The magnitude of J is closely associated with the number of chemical bonds across the related coupled nuclei. Consequently, the number is denoted as an upper left superscript to J , for example, 1J , 2J , and so forth. As the coupling is

conducted through binding electrons, the magnitude of J decreases rapidly with an increase in the number. Thus, the term long-range spin–spin coupling is obtained when the number is greater than a particular integer n . In the ^1H spectra, n is 4 because a coupling across three bonds is common, and n is 2 for the ^{13}C spectra.

The J possesses an algebraic value, which is distinguished by a positive or negative sign. If two coupled nuclei with the same orientation have a higher energy level than that without the coupling, or two coupled nuclei with opposite orientations have a lower energy level than that without the coupling, their J has a positive value. On the other hand, J has a negative value. The absolute value of J can be read or calculated from the related spectrum, but the sign of J is difficult to obtain.

1.4 Magnetization

1.4.1 Magnetization Concept

Since NMR is a phenomenon of an ensemble of magnetic nuclei, it can be discussed from a macroscopic point of view.

In a static magnetic field B_0 , magnetic moments of a particular type of nuclei precess about B_0 along several cones, the number and orientations of which are determined by the spin quantum number I . If $I=1/2$, there are two cones, on which the magnetic moments precess with the same Larmor frequency. According to the Boltzmann's distribution, the population of magnetic moments precessing about B_0 is slightly larger than that of magnetic moments precessing about $-B_0$. Therefore, it could be considered that only the magnetic moments that represent the difference of the two populations precess about B_0 to form a resultant magnetization, as shown in Fig. 1.7.

Suppose that there are N nuclei in a unit volume, we define the magnetization \mathbf{M} as

$$\mathbf{M} = \sum_{i=1}^N \mu_i \quad (1-17)$$

where μ_i is the i -th magnetic moment of a nucleus in a unit volume.

It is clear that

$$\mathbf{M} = \mathbf{M}_{\parallel} + \mathbf{M}_{\perp} \quad (1-18)$$

and

$$\mathbf{M}_{\parallel} = \mathbf{M}_+ + \mathbf{M}_- \quad (1-19)$$

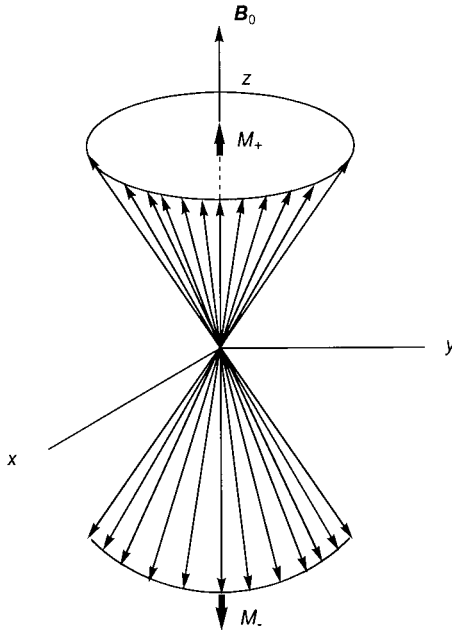


Fig. 1.7 Magnetic moments of nuclei with $l=1/2$ precess on two cones.

where M_{\parallel} and M_{\perp} are the components along B_0 and perpendicular to B_0 , respectively.

If only a static magnetic field exists then

$$M_{\parallel} = M_z = M_+ - M_- \quad (1-20)$$

$$M_{\perp} = 0 \quad (1-21)$$

1.4.2

Rotating Frame

The effect of an oscillating magnetic field (a linear polarized alternating magnetic field), that is, a radiofrequency wave, will now be discussed. A linear polarized alternating magnetic field is composed of two counter-rotating magnetic fields, of which one has the same rotating direction as that of the nuclear magnetic moments. Therefore, the rotating magnetic field with the Lamor frequency can affect the nuclear magnetic moments, and the other rotating magnetic field has no function in NMR.

A laboratory framework consists of three mutually perpendicular axes: the x , the y and the z axes. The last has the same direction as B_0 . Now we will define a rotating frame, in which the z' axis has the same direction as B_0 or the z axis while the x' and the y' axes rotate about the z' axis at the Lamor frequency in the same rotat-

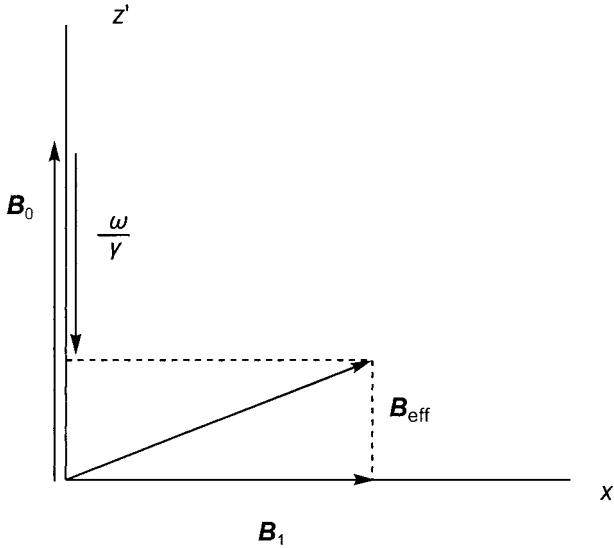


Fig. 1.8 The effective magnetic field, B_{eff} , in the rotating frame.

ing direction as that of the precession of nuclear magnetic moments. In the rotating frame, B_1 is relatively static so that its direction can be set along the x' axis.

By using the rotating frame, the magnetization M can be discussed more easily. M is affected by B_0 along the z' axis and by B_1 along the x' axis. However, since the frame is rotating, a term B_v , known as a virtual field, has to be added to B_0 and B_1 . B_v has the opposite direction to B_0 and its magnitude is given by the following equation:

$$B_v = \omega/\gamma \quad (1-22)$$

where γ is the magnetogyric ratio of the isotope and ω is the rotating frequency of the rotating frame.

M is affected by the resultant magnetic field from B_0 , B_1 and B_v , known as B_{eff} , as shown in Fig. 1.8.

Fig. 1.8 can be expressed by the following equation:

$$B_{\text{eff}} = B_0 + B_v + B_1 \quad (1-23)$$

Since at resonance

$$\omega_0 = \gamma B_0 \quad (1-12)$$

hence

$$B_0 = \omega_0/\gamma$$

where ω_0 denotes the resonant frequency.

Substituting Eq. (1-12) into Eq. (1-23) yields

$$\mathbf{B}_{\text{eff}} = \mathbf{B}_0 + \mathbf{B}_v + \mathbf{B}_1 = [(\omega_0 - \omega)/\gamma]\mathbf{k} + B_1\mathbf{i} \quad (1-24)$$

where \mathbf{k} and \mathbf{i} are the unit vectors of the rotating frame, respectively.

When $\omega = \omega_0$, Eq. (1-24) becomes

$$\mathbf{B}_{\text{eff}} = B_1 \quad (1-25)$$

This equation means that the magnetization \mathbf{M} is affected only by B_1 under the resonant conditions. Therefore, \mathbf{M} will rotate about the x' axis to produce a transverse component, \mathbf{M}_\perp , which is related to an NMR signal. This can be understood as follows: \mathbf{M}_\perp is rotating within the laboratory framework, in which a detection coil is set. The rotating \mathbf{M}_\perp will continuously cut the detection coil to produce a potential, that is, an NMR signal.

If $\omega \neq \omega_0$, the magnetization rotates about the \mathbf{B}_{eff} as given by Eq. (1-24). When $\omega_0 - \omega > B_1$, the magnetization rotates about the z' axis, so that there is no transverse component, that is, no NMR signal.

1.5

Relaxation Process

1.5.1

What is a Relaxation Process?

All types of absorption spectroscopy follow the same principle: sample molecules undergo transitions from a lower energy level to a higher energy level, where the molecules absorb electromagnetic wave quantum with the appropriate energy, which is equal to the difference between the two energy levels. At the same time, some molecules at the higher energy level return to the lower energy level under the same conditions. Because the probability of the transition from the lower energy level to the higher energy level is equal to that of the transition from the higher energy level to the lower energy level, and the population at the lower energy level is slightly greater than that at the higher energy level, according to Boltzmann's distribution law, an absorption signal can be produced. If the absorption signal is to be maintained, some molecules at the higher energy level must be able to return continuously to the lower energy level. This process is known as relaxation. The relaxation in absorption spectroscopy can take place spontaneously. However, its rate is determined by the energy difference between the two energy levels. The smaller the energy difference between the two energy levels, the slower the rate of relaxation. Since NMR transitions have the smallest energy differences in absorption spectroscopy, the relaxation in NMR has to be considered. If the relaxation is not effective, the system will reach saturation, which means the population at the higher energy level is equal to that at the lower energy level, resulting in no NMR signal.

1.5.2

Longitudinal and Transverse Relaxation

Relaxation can be understood more thoroughly through the concept of the magnetization vector \mathbf{M} . When the NMR condition is satisfied, \mathbf{M} (or the cone in Fig. 1.7) tips towards the y' axis of the rotating frame, and correspondingly, the two components of \mathbf{M} change: M_{\parallel} decreases from M_0 to a specific value; M_{\perp} increases from zero to a specific value. As soon as the declination of the magnetization vector begins, the relaxation returns the two components of the magnetization vector to the original (equilibrium) state ($M_{\parallel}=M_0$, $M_{\perp}=0$). Although there are some relationships between the relaxation of M_{\parallel} and that of M_{\perp} , the two relaxations, known as the longitudinal relaxation and the transverse relaxation, respectively, possess different mechanisms and physical significance.

The longitudinal relaxation is the relaxation of the longitudinal component (along the z axis) of the magnetization vector. Before the declination of \mathbf{M} ,

$$M_{\parallel} = M_0 = M_+ - M_-$$

which means M_{\parallel} is associated with the population difference between two related energy levels. From the point of view of energy, nuclear magnetic resonance is a process during which a spin system absorbs some energy from its environment to increase the population of the higher energy level. On the other hand, the longitudinal relaxation returns M_{\parallel} to M_0 so that the population of the higher energy level decreases. This is the process during which the spin system releases some of its energy to its environment. In brief, the longitudinal relaxation is associated with energy exchange between a spin system and its environment. The longitudinal relaxation is also called spin–lattice relaxation, where “lattice” implies the environment.

The transverse relaxation is the relaxation of the transverse component (in the $x'y'$ plane) of the magnetization vector. Prior to nuclear magnetic resonance, magnetic moments of spins precess randomly on the surface of the cone, so that their projections on the $x'y'$ plane have a uniform distribution. There is neither coherence among the phases of the precessing magnetic moments nor a resultant \mathbf{M}_{\perp} . When the resonance takes place, the magnetization vector is declined to create a transverse component on the y' axis (or in the $x'y'$ plane). On the basis of the consideration of the declination of the cone in Fig. 1.7, the projections of precessing magnetic moments form a distribution with a fan-shaped symmetry about the y' axis, which means that the projections of the magnetic moments possess some coherence. The transverse relaxation means that this coherence returns to a uniform distribution. Therefore, the transverse relaxation is an entropy effect.

The inhomogeneity of an applied magnetic field affects the spins of various volume elements with differing magnetic field strengths. Therefore, the inhomogeneity also contributes to the transverse relaxation.

The transverse relaxation is associated with the interactions between the precessing nuclear magnetic moments. It decentralizes their distribution about the

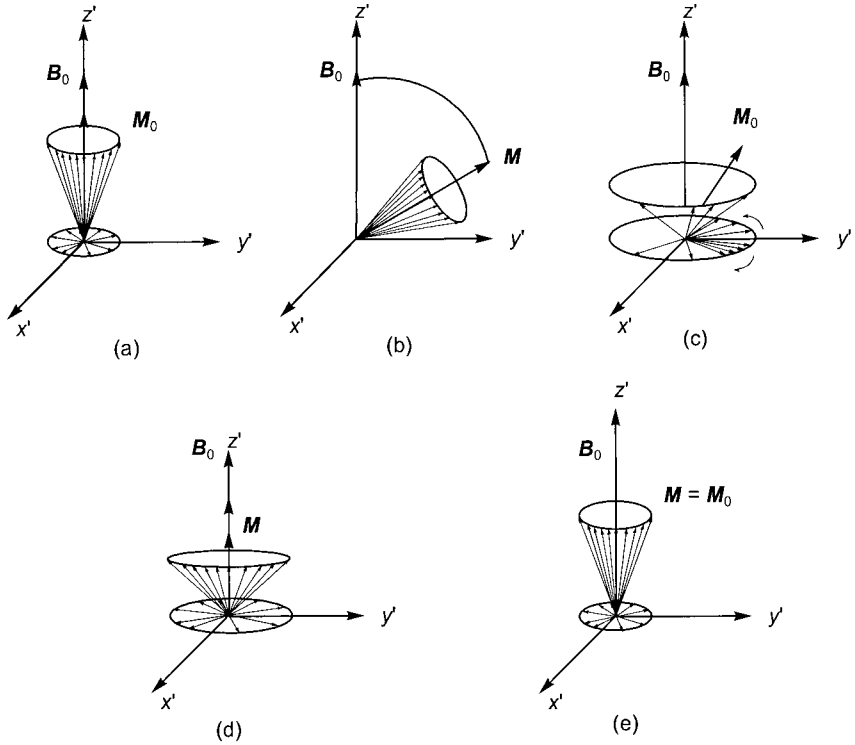


Fig. 1.9 The relaxation process of the magnetization M (a) under equilibrium conditions. (b) M has been declined from the z' axis by the action of B_1 . (c) Both longitudinal relaxation and transverse relaxation take place after the action of B_1 ; the transverse

relaxation is clear. (d) The transverse relaxation has finished and the longitudinal relaxation continues. (e) The longitudinal relaxation has finished; M comes back to the equilibrium condition.

y' axis to attain a uniform distribution about the origin. Consequently, the transverse relaxation is known as spin–spin relaxation.

The rates of the processes of the longitudinal and transverse relaxations are characterized by $1/T_1$ and $1/T_2$, respectively. T_1 and T_2 are similar to the time constant for a first-order chemical reaction. T_1 is the longitudinal relaxation time, and T_2 the transverse relaxation time. Both are measured in seconds.

The two following equations hold:

$$dM_{\parallel}/dt = dM_z/dt = -(M_z - M_0)/T_1 \quad (1-26)$$

$$dM_{\perp}/dt = -(M_{\perp} - 0)/T_2 = -M_{\perp}/T_2 \quad (1-27)$$

where M_0 is the value of M_{\parallel} under the original (equilibrium) conditions; and zero is the value of M_{\perp} under the original (equilibrium) conditions.

When M is declined from the z' axis towards the y' axis, M_{\parallel} decreases while M_{\perp} is formed. After the action of B_1 , M_{\parallel} and M_{\perp} relax with their time constants T_1 and T_2 , respectively, according to Eq. (1-26) or Eq. (1-27). This process is shown in Fig. 1.9, from which it is seen that just at the last moment, M_{\parallel} approaches M_0 , so that $T_1 \geq T_2$.

1.5.3

Width of an NMR Signal

An NMR signal possesses some width because of the uncertainty principle of quantum mechanics.

$$\Delta E \cdot \Delta t \approx h \quad (1-28)$$

where Δt is the duration a particle stays in an energy level, and h is Planck's constant.

In an NMR process, Δt is determined by spin-spin interactions with time constant T_2 . Thus

$$\Delta E \cdot T_2 \approx h \quad (1-29)$$

Since

$$\Delta E = h\Delta\nu$$

one obtains

$$\Delta\nu \approx \frac{1}{T_2} \quad (1-30)$$

The width calculated using Eq. (1-30) is the so-called natural width. Because the inhomogeneity of an applied magnetic field also contributes to the transverse relaxation, apparent transverse relaxation time T_2' is shorter than T_2 . Therefore, Eq. (1-30) becomes

$$\nu \approx \frac{1}{T_2'} \quad (1-31)$$

Consequently, the real line widths measured in NMR experiments are larger than the natural widths.

1.6

Pulse-Fourier Transform NMR Spectrometer

In the past, NMR spectrometers were continuous wave spectrometers, through which an NMR spectrum was recorded by the continuously changing magnetic field strength or radiofrequency (RF). At most only the nuclei of one functional group were resonated at any particular moment in this way. All the other nuclei were waiting for the resonance to occur, so that the sensitivity of the measurement was low.

When there is only a small amount of sample available, it is necessary to repeat the scans to improve the signal-to-noise ratio. The accumulated signal-to-noise ratio is proportional to the square root of the number of scans, \sqrt{n} , because the signal intensity is proportional to n while the noise intensity is proportional to the square root of the number of scans. Since the value of n is rather large and the time for one scan is rather long, the accumulation of data by a continuous wave spectrometer is time-consuming.

To overcome the above-mentioned shortcomings, a new type of NMR spectrometer is required, that is, the pulse-Fourier transform NMR spectrometer.

1.6.1

Application of Strong and Short RF Pulses

In a rotating frame, the effective field of the magnetic nuclei is given by Eq. (1-24), that is:

$$\mathbf{B}_{\text{eff}} = (\omega_0/\gamma - \omega/\gamma)\mathbf{k} + B_1\mathbf{i} \quad (1-24)$$

This equation can be rewritten as:

$$B_{\text{eff}} = \left[\left(\frac{\omega_0}{\gamma} - \frac{\omega}{\gamma} \right)^2 + B_1^2 \right]^{1/2} = \frac{1}{\gamma} [(\omega_0 - \omega)^2 - (\gamma B_1)^2]^{1/2} \quad (1-32)$$

where ω_0 is the resonant frequency of the nuclei; ω is the rotating circular frequency of the frame; and B_1 is the magnetic induction strength of the rotating polarized magnetic field.

The general equation for nuclei with various chemical shifts and coupling constants is

$$B_{\text{eff}} = \frac{1}{\gamma} [(\omega_{0i} - \omega)^2 + (\gamma B_1)^2]^{1/2} \quad (1-33)$$

where B_{eff} is the effective field of the i -th nucleus; and ω_{0i} is the resonant frequency of the i -th nucleus.

Suppose that the spectral width of an NMR spectrum is ΔF (measured in Hertz) and that B_1 is sufficiently strong, so that

$$\gamma B_1 \gg 2\pi\Delta F \quad (1-34)$$

Under these conditions, the second term in the square brackets of Eq. (1-33) can be neglected. Consequently, one has

$$B_{\text{eff}} \approx B_1 \quad (1-35)$$

Eq. (1-35) leads to a very important conclusion: if B_1 is sufficiently strong, all nuclei with different δ and J values have an approximate effective field, B_1 . In other words, all magnetization vectors corresponding to all signals in an NMR spectrum are rotated towards the y' axis under the action of B_1 along the x' axis. Therefore, all nuclei resonate simultaneously although they possess different δ and J values.

As with Eq. (1-13), the rotation of all magnetization vectors about the x' axis can be described by the following equation:

$$\Omega = \gamma B_1 \quad (1-36)$$

where Ω is the angular velocity of M about the x' axis.

Suppose that the duration of the action of B_1 is t_p , during which the rotated angle of M is a , the rotation can be expressed by the following equation:

$$a = \Omega t_p \quad (1-37)$$

Substituting Eq. (1-36) into Eq. (1-37), one obtains:

$$a = \gamma B_1 t_p \quad (1-38)$$

Suppose $a=90^\circ$ (correspondingly, the pulse is known as the $\pi/2$ pulse), Eq. (1-37) becomes

$$\begin{aligned} \pi/2 &= \gamma B_1 t_p \\ t_p &= \frac{\pi}{2\gamma B_1} \end{aligned} \quad (1-39)$$

The substitution of Eq. (1-34) into Eq. (1-39) yields

$$t_p \ll \frac{1}{4\Delta F} \quad (1-40)$$

From Eqs. (1-34) and (1-40), it can be seen that all nuclei can be excited at the same time by using a strong, short pulse.

If Eq. (1-34) can not be satisfied, M will rotate not about B_1 but about B_{eff} , as can be seen from Fig. 1.8.

1.6.2

Time Domain Signal and Frequency Domain Spectrum, and their Fourier Transform

Under the action of a strong, short pulse, all magnetization vectors decline from the x' axis towards the y' axis so their transverse components, the measurable $M_{\perp i}$, are produced. After the action, we have

$$M_{y'_i} = M_{y'_i}(0)e^{-\frac{t}{T_{2i}}} \cos(\omega_{0i} - \omega)t \quad (1-41)$$

where $M_{y'_i}$ is the measured signal of the i -th nucleus at time t ; t is the time recorded at the end of the pulse; $M_{y'_i}(0)$ is the measured signal of the i -th nucleus at $t=0$; T_{2i} is the transverse relaxation time of the i -th nucleus; ω_{0i} is the resonant frequency of the i -th nucleus; and ω is the rotating frequency of the rotating frame.

The term $e^{-t/T_{2i}}$ in Eq. (1-41) originates from the transverse relaxation described by Eq. (1-27). The term $\cos(\omega_{0i}-\omega)t$ arises from the fact that $M_{\perp i}$ rotates in the $x'y'$ plane when $\omega_{0i} \neq \omega$. The signals, $M_{y'_i}$, are termed “free induction decay”, FID, because they are freely precessing transverse components that are induced after the action of pulses and they are being reduced according to their transverse relaxation times. Since each $M_{y'_i}$ has its own ω_{0i} and T_{2i} , the measured signal is an interferogram resulting from the addition of all FIDs. This is a time domain signal since the variable is time. The Fourier transform changes the time domain signal into a frequency spectrum, which we can recognize as follows:

$$F(\omega) = \frac{1}{2\pi} \int_{-\infty}^{\infty} f(t)e^{i\omega t} dt \quad (1-42)$$

Alternatively, the Fourier transform can change a frequency domain spectrum into a time domain signal, that is,

$$\text{FID} = f(t) = \int_{-\infty}^{\infty} F(\omega)e^{i\omega t} d\omega \quad (1-43)$$

In the two equations above, the sign of “ i ” is the imaginary unit.

Because of the different units in Eqs. (1-42) and (1-43), a coefficient, $1/2\pi$, is present in Eq. (1-42).

An intuitive explanation of the Fourier transform is useful to the understanding of abstract calculation. According to the trigonometric expression of a complex number, that is,

$$e^{-i\omega t} = \cos \omega t - i \sin \omega t \quad (1-44)$$

Eq. (1-42) can be rewritten as

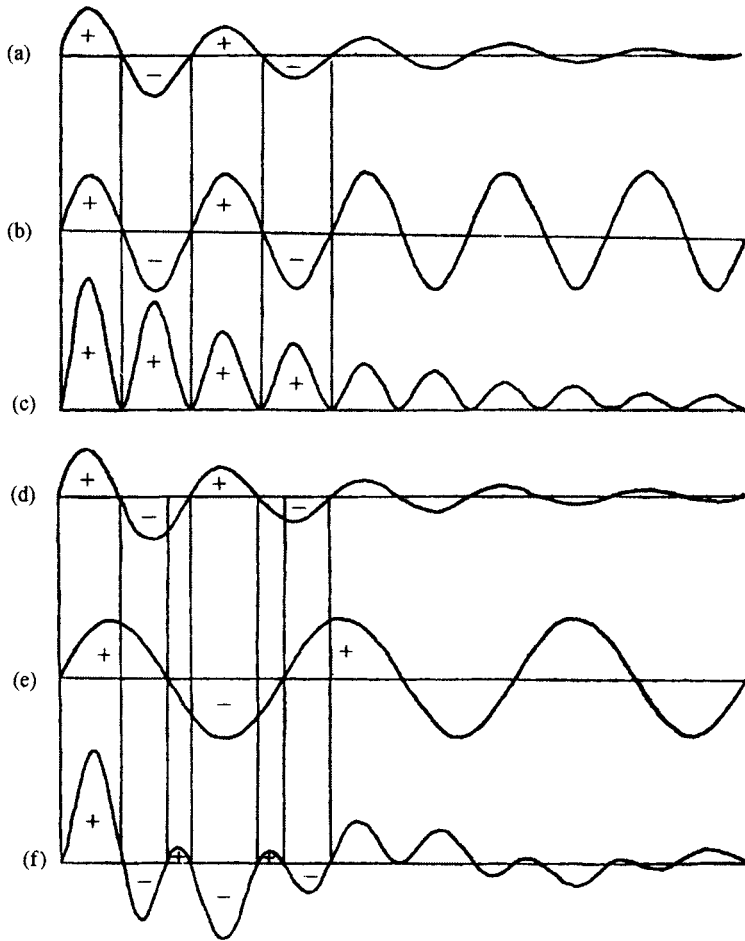


Fig. 1.10 An intuitive explanation of the Fourier transform. (a) $f(t) = \sin \omega'_1 t \times e^{-t/T}$; (b) $\sin \omega_1 t$, $\omega_1 = \omega'_1$; (c) $\sin \omega'_1 t \times e^{-t/T} \times \sin \omega_1 t$; (d) $f(t) = \sin \omega'_2 t \times e^{-t/T}$; (e) $\sin \omega_2 t$, $\omega_2 = (3/5)\omega'_2$; (f) $\sin \omega'_2 t \times e^{-t/T} \times \sin \omega_2 t$.

$$F(\omega) = \frac{1}{2\pi} \int_{-\infty}^{\infty} f(t) [\cos \omega t - i \sin \omega t] dt \quad (1-45)$$

A real and an imaginary component can be obtained from Eq. (1-45).

Now $\int_{-\infty}^{\infty} f(t) \sin \omega t dt$ will be used as an example. Similarly, we can calculate the other component since $\cos \omega t = \sin(\omega t + \pi/2)$.

The calculation of $\int_{-\infty}^0 f(t) \sin \omega t dt$ can be understood from Fig. 1.10.

If ω' in $f(t) = \sin \omega' t \times e^{-t/T}$ is equal to ω in $\sin \omega t$ and both $f(t)$ and $\sin \omega t$ have the same phase, the product of every component is positive. Therefore, the integration, which is the addition of all products, is positive, that is, it has a non-zero value.

On the other hand, if $\omega' \neq \omega$, then some products are positive and some are negative leading to an integration of zero, which can be proved strictly by mathematics.

$f(t)$ is an addition of FIDs with many frequencies. A spectral width will be set for a spectral recording. An ω value, which is varied gradually and discontinuously from one end to another of the spectral width, is taken for the calculation of the Fourier transform. If this ω is equal to an ω' in FIDs, a non-zero integral value is obtained. Consequently, a peak is present in an NMR spectrum. On the other hand, if any ω' of FIDs is not equal to the ω , the integral value is zero, that is, there is no peak at the position of the abscissa, ω . An NMR spectrum is obtained after the discontinuous calculation for the spectral width to be set.

1.6.3

FT-NMR with Respect to the Fourier Decomposition

FT-NMR can be understood from another point of view, that is, from the Fourier decomposition.

A square waveform can be decomposed into a series of harmonic components, as shown in Fig. 1.11.

From Fig. 1.11 it can be seen that the more harmonic components are added, the nearer the result of the addition approaches the square waveform. If the number of components increases to infinity, the addition forms the square waveform. It can be assumed that a sample can “perceive” infinite frequencies under the action of a pulse with a square waveform, which means that nuclei with different resonant frequencies can resonate simultaneously through a single pulse.

However, the discussion above is only an explanation in principle. If an NMR experiment uses a pulse as shown in Fig. 1.11, amplitudes of effective components are too weak.

The NMR experiment applies an electromagnetic wave modulated by rectangular pulses, which is shown in Fig. 1.12.

The modulation means that one function is multiplied by another function. Through the physical concepts, a sample can perceive many discrete frequencies positioned within a wide range of frequencies, as shown in (c) of Fig. 1.11.

The envelope curve of the amplitudes of frequency components is expressed by the following equation:

$$H(f - f_0) = \frac{A t_p \sin[\pi(f - f_0)t_p]}{PD\pi(f - f_0)t_p} \quad (1-46)$$

where $H(f - f_0)$ is the intensity of the component with a frequency of $(f - f_0)$; A is the intensity of the rectangular pulse; PD is the cycle of the rectangular pulse; and t_p is the duration of the rectangular pulse.

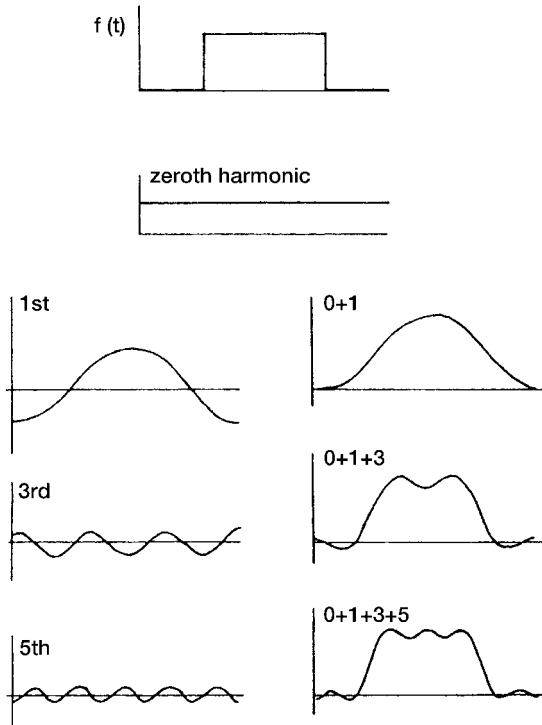


Fig. 1.11 A square waveform is an addition of a series of harmonic components. Reprinted from reference [2], with permission from Elsevier.

From Fig. 1.12 d or Eq. (1-46), it is clear that $H(f - f_0) = 0$ when $(f - f_0) = 1/t_{p0}$. Because t_p is very short (several microseconds), $(f - f_0)$ with an amplitude greater than zero has a very large range. If $(f - f_0) \ll 1/t_p$ (which is the case in practice), the $H(f - f_0)$ values are very close to $H(f_0)$, which means that the NMR signals have perfect quantitative relationships in spite of their different resonant frequencies.

The frequency interval between every two components is equal to $1/PD$, which is generally less than the width of an NMR signal, so that the NMR signals cannot be missed.

FT-NMR has been discussed in the two previous sections. In fact, these two arguments are related, but each stresses one of the two sides accordingly.

The first argument, covering the equations from (1-32) to (1-40), gives a clear explanation of the necessity of a pulse with strong power and of a short duration. Under the conditions with $(\gamma B_1)^2 \gg (\omega_{0i} - \omega)^2$, all nuclei in different functional groups resonate simultaneously and they have approximately quantitative signals.

The second argument, discussed in Section 1.6.3, explicates intuitively the frequency distribution of a pulse. As a short t_p , during which the energy transmission for the nuclei is achieved, is necessary to obtain a good quantitative result, it could be understood that the power of the pulse must be strong.

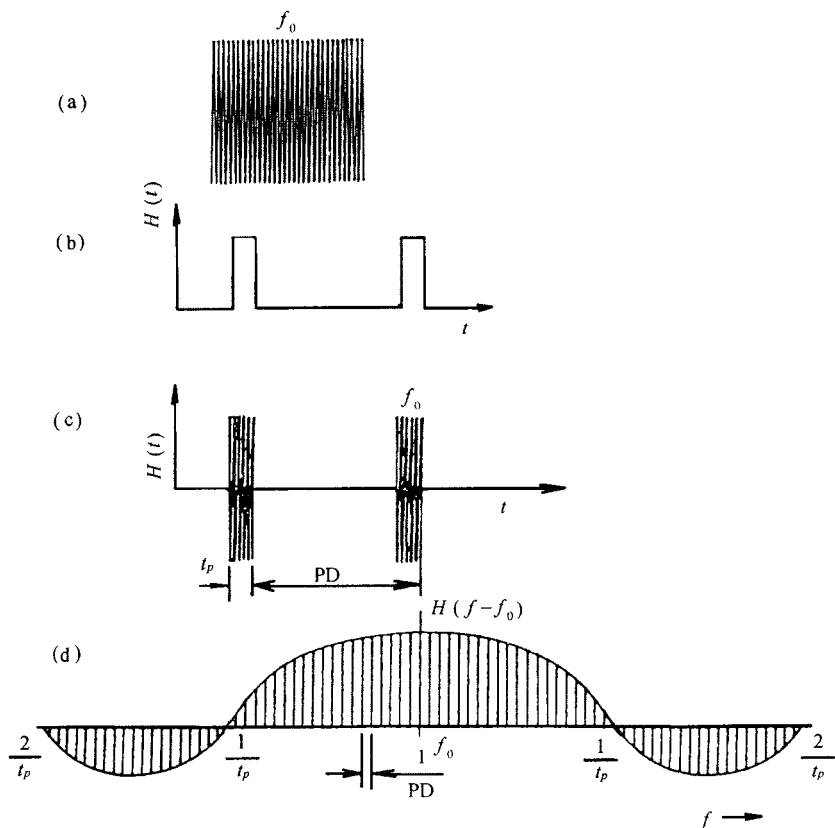


Fig. 1.12 The principle of pulse-FT-NMR. (a) A continuous RF wave with a frequency f_0 of equi-amplitude. (b) Periodic square

pulses. (c) The result of (a) modulated by (b). (d) Discrete frequency components obtained by (c).

Now return to the first argument, which is based on the rotating frame with a rotating frequency f_0 , which is just the center of the frequency distribution in Fig. 1.12d. In addition, ΔF in Eq. (1-34) corresponds to the chosen frequency width in the broad frequency distribution. Therefore, these two arguments are actually related.

1.6.4

Advantages of an FT-NMR Spectrometer

The change from continuous wave (CW) NMR spectrometers to FT-NMR spectrometers was a milestone for NMR instruments. FT-NMR spectrometers have many advantages over CW NMR spectrometers. The main advantages are as follows:

1. All nuclei in different functional groups are simultaneously in resonance, which greatly improves the efficiency of NMR measurements.

2. Since the repeat time of pulses is short (less than several seconds in general), an accumulation of data acquisition can be accomplished in a time much shorter than that by CW NMR spectrometers.
3. For the FT-NMR spectrometer, its pulse emission and data acquisition are carried out according to a time-sharing system so that the energy leakage from the emitter into the receptor, which occurs in CW spectrometers, is removed.
4. Pulse sequences, by which 2D NMR experiments are created, can only be used in FT-NMR spectrometers.

On the basis of 1, 2 and 3, NMR measurements with FT-NMR spectrometers can be accomplished with a much smaller amount of sample and/or in a much shorter time compared with CW spectrometers. The application of pulse sequences has led to a significant evolutionary stage in NMR spectroscopy: from one-dimensional NMR spectra into multi-dimensional NMR spectra.

1.7

Recent Developments in NMR Spectroscopy

The main progress in NMR spectroscopy has been associated with the application of pulse sequences. This will be described in Chapter 4.

NMR measurements with micro-quantities of samples will be discussed in Section 9.3.3.

LC-NMR, the latest hyphenated technique between a separation system and an analytical instrument, will now be presented. The combination of the superior separation capabilities of HPLC with the exceptional structural elucidation capabilities of NMR forms a powerful and versatile tool for examining the chemical structures of a complex mixture. For example, both the identification of several known alkaloids and the characterization of new chemical structures are possible without previous isolation and purification [3].

The LC-NMR instrument consists of an HPLC system and an NMR spectrometer with a flow cell, which has a very small volume (e.g. 60 μL). LC-NMR is more difficult than LC-MS, in which the solvent is removed before MS measurements. However, in LC-NMR experiments, the solvents, the peak intensities of which are much stronger than those of samples, by several orders of magnitude, cannot be removed. Even the ^{13}C satellites are much stronger than the signals of the solutes. In addition, because of the application of gradient elution, the solvent peaks will shift in the course of the elution, which means that researchers are confronted with moving targets. Therefore, the suppression of the solvent peaks is the most critical task in LC-NMR. The low sensitivity of NMR is another difficulty for LC-NMR. However, the following developments have led to the practical application of LC-NMR.

1. The frequency used in NMR spectrometers has been raised to 920 MHz, which considerably improves the sensitivity. In practice, an NMR spectrometer with a frequency of higher than 500 MHz is suitable for LC-NMR.

2. On the basis of shaped pulses (see Section 4.1.10) and pulsed field gradients (see Section 4.1.9), effective techniques for solvent suppression have been developed. Some of these are termed “excitation sculpting” [4], from which their function can be understood. LC-NMR experiments can now be carried out without deuterated organic solvents, which are very expensive.
3. The progress in automation and software has made the process of LC-NMR easier.

Our attention will now focus on the suppression of solvent peaks.

There are two types of LC-NMR experiment: continuous-flow (on-flow) monitoring and stop-flow monitoring (which includes using loops to store samples). The monitoring of LC-NMR in real time can be achieved in the on-flow mode but 2D NMR spectra of LC-NMR can only be recorded in the stop-flow mode.

From the point of view of hyphenated instruments, the continuous-flow (on-flow) mode is ideal. However, it is restricted to measuring ^1H spectra because of its low sensitivity.

WET (water suppression enhanced through the T_1 effect) [5, 6] is usually applied in LC-NMR. The WET sequence consists of several shaped RF pulses, which are aimed at the various solvent frequencies that need to be suppressed. Each shaped RF pulse follows a pulsed field gradient and a short delay to dephase a transverse magnetization vector of solvents. In this way, five or more of the solvent peaks can be suppressed. In addition, selective ^{13}C decoupling suppresses the ^{13}C satellites.

When LC-NMR is manipulated in the on-flow mode, scout scans are applied. A scout scan is a one-transient, one-pulse experiment to locate the positions of the solvent peaks. Special software then adjusts the transmitter so as to point to the largest solvent peak and keeps this position at a constant frequency. Once the solvent peak position is determined by the scout scan, an adjusted solvent peak suppression is executed and acquisitions are accumulated. The process is then repeated.

In addition to LC-NMR, there is also LC-NMR-MS, SFC (supercritical fluid chromatography)-NMR, and so forth.

The analysis of a mixture can be achieved without separation by using DOSY (diffusion ordered spectroscopy) which will be described in Section 4.13.

1.8

References

- 1 T. C. FARRAR, E. D. BECKER, *Pulse and Fourier Transform NMR, Introduction to Theory and Methods*, Academic Press, 1971.
- 2 D. SHOW, *Fourier Transform N.M.R. Spectroscopy* (Second Edition), Elsevier, 1984.
- 3 G. BRINGMANN, C. GUNTHER et al., *Anal. Chem.* **1998**, *70*, 2805–2811.
- 4 T. L. HWANG, A. J. SHAKE, *J. Magn. Reson. A* **1995**, *112*, 275–279.
- 5 H. S. SMALLCOMBE, S. L. PATT et al., *J. Magn. Reson. A* **1995**, *117*, 295–303.
- 6 R. J. OGG, P. B. KINGSLEY et al., *J. Magn. Reson. B* **1994**, *104*, 1–10.